In vivo imaging reveals that pregabalin inhibits cortical spreading depression and propagation to subcortical brain structures

Cain, S.M.; Bohnet, B.; Ledue, J.; Yung, A.C.; Garcia, E.; Tyson, J.R.; ... ; Snutch, T.P.

In vivo imaging reveals that pregabalin inhibits cortical spreading depression and propagation to subcortical brain structures

Stuart M. Cain[a,b,1], Barry Bohnet[c], Jeffrey LeDue[b], Andrew C. Yung[c], Esperanza Garcia[a,b], John R. Tyson[a,b], Sascha R. A. Alles[a,b], Huili Han[b], Arn M. J. M. van den Maagdenberg[d,e], Piotr Kozlowski[c], Brian A. MacVicar[b], and Terrance P. Snutch[a,b,1]

[a]Michael Smith Laboratories, University of British Columbia, Vancouver, BC V6T 1Z4, Canada; [b]Djavad Mowafaghian Center for Brain Health, University of British Columbia, Vancouver, BC V6T 1Z4, Canada; [c]UBC MRI Research Centre, University of British Columbia, Vancouver, BC V6T 1Z4, Canada; [d]Department of Human Genetics, Leiden University Medical Center, 2300 RC Leiden, The Netherlands; and [e]Department of Neurology, Leiden University Medical Center, 2300 RC Leiden, The Netherlands

Edited by Kurt G. Beam, University of Colorado Denver, Anschutz Medical Campus, Aurora, CO, and approved December 29, 2016 (received for review August 29, 2016)

Migraine is characterized by severe headaches that can be preceded by an aura likely caused by cortical spreading depression (SD). The antiepileptic pregabalin (Lyrica) shows clinical promise for migraine therapy, although its efficacy and mechanism of action are unclear. As detected by diffusion-weighted MRI (DW-MRI) in wild-type (WT) mice, the acute systemic administration of pregabalin increased the threshold for SD initiation in vivo. In familial hemiplegic migraine type 1 mutant mice expressing human mutations (R192Q and S218L) in the $Ca_V2.1$ (P/Q-type) calcium channel subunit, pregabalin slowed the speed of SD propagation in vivo. Acute systemic administration of pregabalin in vivo also selectively prevented the migration of SD into subcortical striatal and hippocampal regions in the R192Q strain that exhibits a milder phenotype and gain of $Ca_V2.1$ channel function. At the cellular level, pregabalin inhibited glutamatergic synaptic transmission differentially in WT, R192Q, and S218L mice. The study describes a DW-MRI analysis method for tracking the progression of SD and provides support and a mechanism of action for pregabalin as a possible effective therapy in the treatment of migraine.

familial hemiplegic migraine type 1 | migraine | diffusion-weighted MRI | voltage-gated calcium channel | gabapentinoids

Migraine is a common debilitating episodic brain disorder that presents as severe headaches accompanied by other symptoms including nausea and vomiting. In approximately one-third of patients the headache phase is preceded by an aura, thought to be caused by cortical spreading depression (SD) (1). SD is characterized by electrocorticographic silencing and a directly coupled potential shift that is generated by spreading neuronal and glial depolarization. In addition to the aura in migraine, SD is associated with various pathological conditions, such as epilepsy, ischemic stroke, and subarachnoid hemorrhage (2–4). The SD wave front of brief neuronal excitation is followed by a long-lasting depolarization and travels rostrally at a speed of 2–6 mm/min, rendering invaded tissue inactive (5). SD induces cell swelling and the release of various neuroactive factors, including glutamate, potassium, protons, and prostaglandins that together contribute to the pathophysiological process (4). A clue to the importance of SD in migraine comes from the observation that in experimental models cortical SD triggers downstream headache mechanisms through the activation of trigeminal nerves and brainstem nuclei (6).

Familial hemiplegic migraine (FHM) is a monogenic form of migraine with aura accompanied by hemiparesis (1). FHM type 1 (FHM-1) is caused by missense mutations in the *CACNA1A* gene that encodes the α_{1A} subunit of voltage-gated $Ca_V2.1$ (P/Q-type) calcium channels (7). FHM-1 mutations introduced into the orthologous *Cacna1a* gene produce transgenic mice with phenotypes that closely mimic both the milder (R192Q) and more severe (S218L) symptoms described in FHM-1 patients with these mutations (8, 9). FHM-1 mutations have been shown to produce an overall gain-of-function increase in calcium conductance at physiological membrane potentials (10, 11); given the well-established role of the channels in the calcium-mediated release of vesicular neurotransmitters, this increase can explain the increased synaptic activity observed in the mutant animals (12–16).

Although a number of preventative and abortive treatments are available, not all migraines are effectively treated, and hospitalization can be necessary for prolonged migraine attacks (2, 17). Gabapentinoids (gabapentin and pregabalin) are small-molecule drugs used clinically in the treatment of neuropathic pain and partial seizures. Gabapentin was initially designed as a GABA analog, and pregabalin was developed to modulate GABA metabolism with the aim of generating new treatments for epilepsy. Instead, these drugs were shown to bind to the $\alpha_2\delta_{1/2}$ subunits of high-voltage–activated calcium channels with little direct effect on either GABA receptors or metabolism (18). Although, initial studies suggested that gabapentin may be effective in the treatment of migraine, it has since been shown to have only nominal potency in migraineurs (19). Pregabalin (Lyrica) displays more linear kinetics and a longer half-life than gabapentin (20) and has shown initially encouraging results as a potential treatment for migraine

Significance

Spreading depression is proposed to underlie migraine with aura, a type of debilitating headache for which few pharmacological treatments are available. The pain drug pregabalin has demonstrated initial promising results for the treatment of migraine in the clinic. Utilizing animal models of congenital migraine and live brain imaging, we describe the cortical and subcortical migration of the spreading depression wave. Further, pregabalin is shown to be effective at suppressing spreading depression initiation, wave speed, and subcortical propagation, and also to affect nerve cell signalling directly. Overall, the study supports the therapeutic potential of pregabalin in both noncongenital migraineurs and patients with mild congenital migraine.

Author contributions: S.M.C., B.B., A.C.Y., E.G., P.K., B.A.M., and T.P.S. designed research; S.M.C., B.B., A.C.Y., E.G., S.R.A.A., and H.H. performed research; S.M.C., B.B., J.L., A.C.Y., J.R.T., A.M.J.M.v.d.M., P.K., and B.A.M. contributed new reagents/analytic tools; S.M.C., B.B., J.L., A.C.Y., E.G., S.R.A.A., and H.H. analyzed data; and S.M.C. and T.P.S. wrote the paper.

Conflict of interest statement: This project was supported in part by the Pfizer Neuropathic Pain Award, and Pregabalin was donated by Pfizer.

This article is a PNAS Direct Submission.

Freely available online through the PNAS open access option.

See Commentary on page 2112.

[1]To whom correspondence may be addressed. Email: scain@msl.ubc.ca or snutch@msl.ubc.ca.

This article contains supporting information online at www.pnas.org/lookup/suppl/doi:10.1073/pnas.1614447114/-/DCSupplemental.

(21–23), although additional evidence of clinical efficacy is required. Although pregabalin's exact mechanism of action has not been deciphered, it has been shown to inhibit calcium currents acutely (24) and to suppress calcium channel trafficking chronically (25). Furthermore, pregabalin displays greater efficacy for P/Q-type ($Ca_V2.1$) channels than for L-type ($Ca_V1.1$-$Ca_V1.4$) and N-type ($Ca_V2.2$) channels (26). Although there is some controversy about the putative acute versus chronic molecular mechanisms, pregabalin has been associated convincingly with a reduction in excitatory neurotransmitter release, further implicating $Ca_V2.1$ calcium channels (27).

Here we examined FHM-1 mouse models to determine the effects of pregabalin on the threshold for SD initiation and the propagation speed of the SD wave front in vivo using a newly developed, customized DW-MRI methodology. Using this method of DW-MRI analysis, we were able to track the spread of SD through the brain with proficient spatiotemporal accuracy. Furthermore, we correlated the findings on SD with in vitro analysis of pregabalin efficacy in acute brain slices using intrinsic optical signaling (IOS) and with spontaneous and evoked synaptic activity in the hippocampus.

Results

Pregabalin Increases the Threshold for SD in WT Mice in Vivo. To examine the full potential of our DW-MRI methodology in the intact brain and in response to pregabalin administration, anesthetized mice were scanned using DW-MRI to visualize the spread of SD in vivo. DW-MRI images were acquired as eight consecutive slices at 8-s intervals for 13 min. SD was initiated using dual carbon fiber electrodes implanted in the occipital cortex (Fig. 1*A* and Fig. S1). Vehicle-treated WT and R192Q mice did not display a significant difference in SD threshold (WT vs. R192Q: $P = 0.21$, ANOVA), but the threshold was significantly lower in vehicle-treated S218L mice (WT vs. S218L: $P = 0.02$; R192Q vs. S218L: $P = 0.03$ ANOVA) (Fig. 1*B*). Subsequently, scans were acquired in WT and FHM-1 mice following the administration of pregabalin (160 mg/kg i.p. 45–60 min before scanning). Pregabalin treatment significantly increased the SD threshold in WT mice; although a trend toward an increased threshold was observed in the R192Q and S218L groups, a significant difference was not achieved for the FHM-1 strains (WT control vs. WT pregabalin: $P = 0.03$, t test; R192Q control vs. R192Q pregabalin: $P = 0.14$, t test; S218L control vs. S218L pregabalin: $P = 0.15$ t test) (Fig. 1*B*).

The sequential DW-MRI slices and 8-s temporal resolution allowed tracking of the SD wave trajectory across the cortex. SD was first visible in slice 3 (bregma −5.00) corresponding to the electrode position in the occipital cortex (Fig. S1), and from this point the wave front traveled both around the circumference of the cortex and rostrally until reaching slice 8, the last slice acquired in the frontal cortex (Movies S1–S3). Of note, the SD wave front did not invade the cerebellum (slices 1 and 2) (Fig. S1*D*) in either the WT ($n = 5$) or FHM-1 ($n = 12$) strains. SD could not be initiated in cerebellum even when stimulation electrodes were placed directly in the vermis of the cerebellar cortex, suggesting that this region is refractory to SD ($n = 1$).

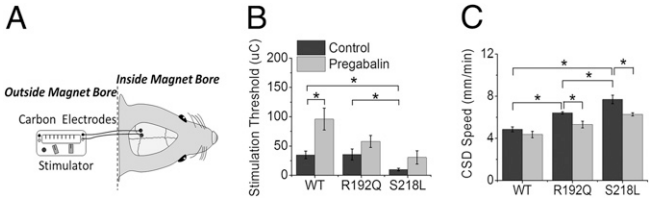

Fig. 1. DW-MRI in vivo. (*A*) Diagram showing the setup for DW-MRI scanning. (*B*) Mean in vivo data for the SD stimulation threshold in vehicle- and pregabalin-pretreated mice: WT control = 35.0 ± 6.5 μC ($n = 5$); R192Q control = 35.8 ± 9.3 μC ($n = 6$); S218L control = 10.0 ± 2.2 μC ($n = 6$); WT pregabalin = 96.0 ± 18.6 μC ($n = 5$); R192Q pregabalin = 58.0 ± 10.2 μC ($n = 5$); S218L pregabalin = 30.6 ± 11.4 μC ($n = 8$). (*C*) Mean data for wave-front speed: WT control = 4.9 ± 0.2 mm/min ($n = 5$); R192Q control = 6.4 ± 0.1 mm/min ($n = 6$); S218L control = 7.7 ± 0.4 mm/min ($n = 6$); WT pregabalin = 4.4 ± 0.3 mm/min ($n = 5$); R192Q pregabalin = 5.3 ± 0.3 mm/min ($n = 5$); S218L pregabalin = 6.3 ± 0.1 mm/min ($n = 8$). *$P < 0.05$, one-way ANOVA with Tukey's post hoc test (between strains) and paired sample t test (control versus pregabalin treatment).

Pregabalin Slows SD Speed in R192Q and S218L FHM-1 Mutant Mice in Vivo. SD speed was calculated from the cortex as the wave front traveled from slice 5 to slice 8. Both R192Q and S218L mice displayed a faster SD than WT mice, and the speed was faster in S218L mice than in R192Q mice (WT vs. R192Q: $P = 0.04$; WT vs. S218L: $P = 0.001$; R192Q vs. S218L: $P = 0.02$, ANOVA) (Fig. 1*C* and Movies S1–S3). Notably, pregabalin treatment slowed SD speed significantly in both R192Q and S218L strains but had no effect in WT mice (WT control vs. WT pregabalin: $P = 0.23$; R192Q control vs. R192Q pregabalin: $P = 0.003$; S218L control vs. S218L pregabalin: $P < 0.0001$, t test) (Fig. 1*C* and Movies S4–S6).

A previous report found that SD is constrained to the cortex in WT mice but can invade the striatum in R192Q mice and can invade the striatum, hippocampus, and, occasionally, thalamus in S218L mice (28). Our data generally are in line with these findings, except that we did not observe SD invasion of the thalamus in S218L animals (Figs. 2 and 3 and Movies S1–S3). Of note, in R192Q mice we observed that SD invaded both the hippocampus and striatum, albeit with a significant delay of up to 1 min after the SD wave front had passed through the cortex. In contrast, in S218L mice the SD wave front moved into cortical and subcortical structures almost simultaneously, consistent with the larger gain-of-function effect of this mutation. Notably, although pregabalin did not prevent the invasion of subcortical structures in S218L mice, it completely abolished spread into both striatum and hippocampus in four of five R192Q mice tested (Figs. 2 and 3 and Movies S2, S3, S5, and S6).

For further visualization and quantitative comparisons of DW-MRI images during SD enhance, a custom Matlab script was designed to detect the SD wave front automatically and to represent it in each slice as a heatmap in which cold colors correspond to early and hot colors to late SD appearance. Representative examples shown in Fig. S2 emphasize the cortical confinement of SD in WT mice and the subcortical invasion in FHM-1 mice. Furthermore, they confirm the marked delay in the arrival of the SD wave front in striatum and hippocampus of R192Q mice. Finally, this image analysis tool confirmed that pregabalin administration slows SD speed in both strains of FHM-1 mice and prevents subcortical invasion of SD in R192Q mice.

Pregabalin Slows the Speed of SD in S218L Mutant Brain Slices in Vitro. To examine the effects of pregabalin on SD further, we used IOS imaging on acute brain slices from FHM-1 and WT mice. In this preparation SD is visualized as an increase in brightness resulting from the increased transparency of the brain tissue caused by cell swelling during the depolarization (29). Bath application of 40 mM KCl induced SD in brain tissue, occasionally from more than one focal point (Fig. 4). The SD wave front traveled across the cortex and invaded (and sometimes was initiated in) the caudate putamen in brain slices from both FHM-1 and WT mice (Fig. 4*A*). In agreement with previous findings (8, 9), the speed of the cortical SD wave front was significantly faster in brain slices from R192Q and S218L animals than in slices from WT mice (WT vs. R192Q: $P = 0.01$, ANOVA; WT vs. S218L: $P = 0.001$, ANOVA) (Fig. 4 *A* and *B*). Pregabalin pretreatment (1 h) had no significant effect on SD speed in brain slices from WT mice, but it significantly slowed SD speed in brain slices from both R192Q and S218L animals (WT control vs. WT pregabalin: $P = 0.26$, t test; R192Q control vs. R192Q pregabalin: $P = 0.03$, t test; S218L control vs. S218L pregabalin: $P = 0.0005$, t test) (Fig. 4*B*). No significant difference in the degree of localized cell swelling correlated with ΔIOS (29) was observed either among strains or as a result of pregabalin pretreatment (Fig. 4*C*).

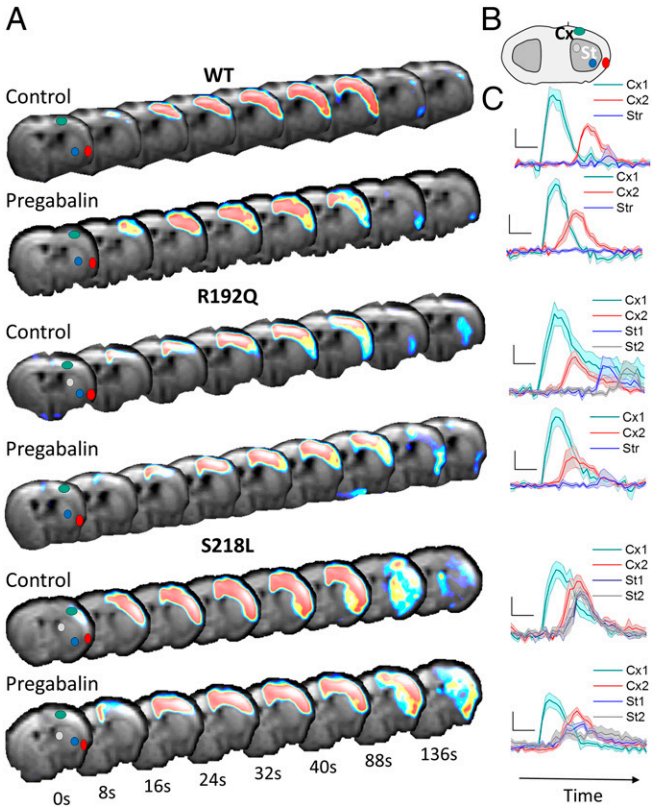

Fig. 2. Cortical–striatal SD spread in WT and FHM-1 mice. (*A*) Representative coronal DW-MRI images at the level of the striatum (bregma −1.25 mm) with superimposed images of pixel intensity during SD. (*B*) Coronal map corresponding to DW-MRI images in cortex (Cx) and striatum (St). (*C*) Time course plots of SD spread showing the mean pixel intensity in regions of interest (ROIs) defined in *A* and the in the coronal map in *B*. (Scale bars, 50 s or 10 arbitrary units.)

Pregabalin Acutely Inhibits $Ca_V2.1$ Calcium Channel Complexes Containing the $\alpha_2\delta_1$ Subunit. To confirm pregabalin's effects on $Ca_V2.1$-mediated calcium currents, electrophysiological recordings were performed in human-derived neuroblastoma SH-SY5Y cells transiently expressing the recombinant human $Ca_V2.1$ subunit coexpressed with β_2 and either $\alpha_2\delta_1$ or $\alpha_2\delta_3$ auxiliary subunits. The effect of pregabalin pretreatment was assessed at a concentration of 500 μM, previously reported to inhibit synaptic activity in the mouse brainstem auditory system (30). The peak calcium current amplitude elicited by repetitive square depolarizations from a holding potential of −110 mV to 0 mV was reduced by 27% ($n = 8$) when 500 μM pregabalin was applied to SH-SY5Y cells expressing $Ca_V2.1$ cotransfected with the β_2 and $\alpha_2\delta_1$ subunits (Fig. 5*A*). Conversely, currents obtained upon coexpression with the β_2 and $\alpha_2\delta_3$ subunits were unaffected by pregabalin (Fig. 5*A*). The selective inhibitory effect on $Ca_V2.1$ channels coexpressed with the $\alpha_2\delta_1$ but not with the $\alpha_2\delta_3$ ancillary subunit was observed across a range of voltage steps elicited by a current–voltage relationship (Fig. 5*B*). These results are consistent with gabapentinoids' higher binding affinity for the $\alpha_2\delta_1$ subunit than for the $\alpha_2\delta_3$ subunit (31).

Pregabalin Suppresses Spontaneous and Evoked Synaptic Activity. We next examined whether the effects of pregabalin on intrinsic neuronal excitability and/or synaptic activity levels could explain the differential alterations in the threshold and speed of SD in WT and FHM-1 mice. Whole-cell patch-clamp recordings in hippocampal acute slices were used because the DW-MRI analyses revealed that SD invasion occurred in this region in S218L and R192Q mice but not in WT mice. Potential differences in global hippocampal synaptic activity were investigated by recording spontaneous excitatory postsynaptic currents (sEPSCs) (see Fig. S4*B*) in the absence of any stimulation or current injection, using whole-cell voltage-clamp recordings with picrotoxin in the patch pipette to block GABAergic inhibitory PSCs (IPSCs). Pregabalin (500 μM) significantly reduced the amplitude and increased the sEPSC interval (i.e., decreased the sEPSC frequency) in CA1 neurons in slices from both WT and R192Q mice (Fig. 5 *C* and *D* and Figs. S3 and S4*A*). Rather unexpectedly, pregabalin was found to increase amplitude and decrease the interevent interval in S218L CA1 neurons. At a lower concentration (100 μM) pregabalin had no effect on sEPSC amplitude or frequency in WT neurons, reduced the frequency of sEPSCs in both R192Q and S218L neurons, and increased the amplitude of sEPSCs in S218L CA1 neurons (Fig. 5*E* and Fig. S4*A*).

To examine the effect of pregabalin on electrically evoked EPSPs (eEPSPs) in hippocampal slices, a paired-pulse stimulation protocol was applied to glutamatergic CA3 axons (Schaffer collaterals) while simultaneously recording voltage responses using current-clamp recordings in CA1 soma (Fig. 5*F*). To ameliorate cell-to-cell variability, eEPSP amplitude was normalized to the control eEPSP peak. Although pregabalin (500 μM) significantly reduced the amplitude of eEPSPs in both WT and R192Q neurons, it had no significant effect on S218L CA1 neurons. At a lower concertation (100 μM), pregabalin inhibited eEPSP amplitude only in R192Q CA1 neurons. No significant effect of pregabalin was observed on paired-pulse facilitation (Fig. 5*F*).

Discussion

One aim of this study was to develop advanced neuroimaging methodologies that permit the in vivo visualization of SD in a

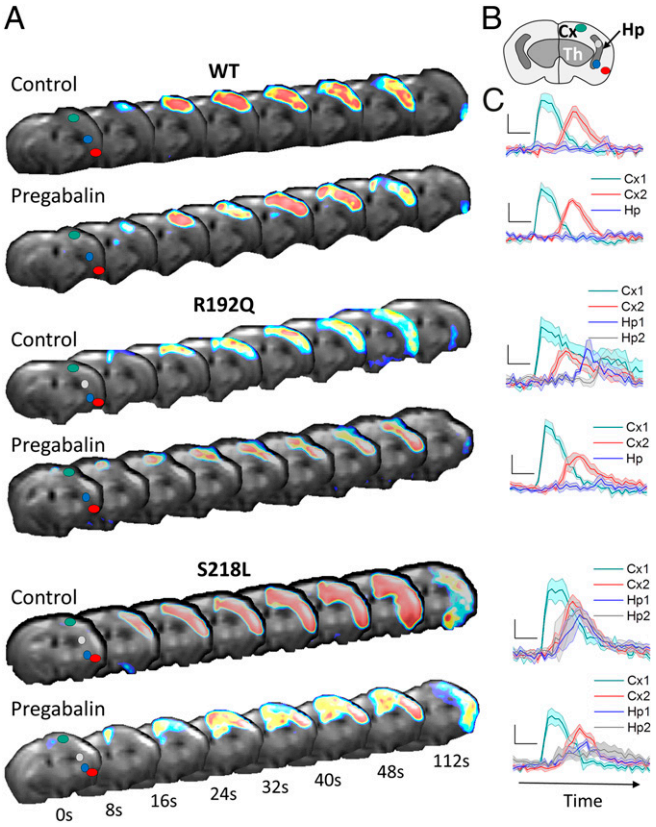

Fig. 3. Cortical–hippocampal SD spread in WT and FHM-1 mice. (*A*) Representative coronal DW-MRI images at the level of the hippocampus (bregma −2.5 mm) with superimposed images of pixel intensity during SD. (*B*) Coronal schematic corresponding to DW-MRI images in cortex (Cx), hippocampus (Hp), and thalamus (Th). (*C*) Time course of SD spread showing mean pixel intensity in the ROIs in *A* and *B*. (Scale bars: horizontal, 50 s; vertical, 10 arbitrary units.)

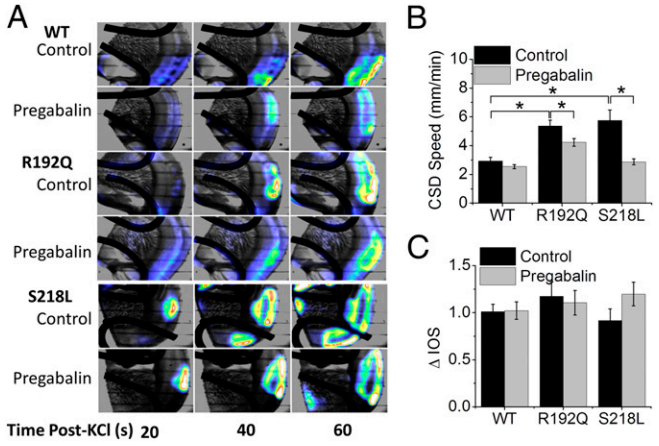

Fig. 4. IOS imaging in acute coronal brain slices. (*A*) Representative images of brain slices from WT, R192Q, and S218L mice following KCl (40 mM) application to initiate SD. (*B*) Mean IOS data for SD wave-front speed: WT control: 2.9 ± 0.3 mm/min (n = 20); R192Q control: 5.4 ± 0.4 mm/min (n = 16); S218L control: 5.8 ± 0.7 mm/min (n = 14); WT pregabalin: 2.5 ± 0.1 mm/min (n = 14); R192Q pregabalin: 4.2 ± 0.3 mm/min (n = 14); S218L pregabalin: 2.9 ± 0.9 mm/min (n = 13). (*C*) Mean data for the ΔIOS signal in control and pregabalin-pretreated brain slices. *P < 0.05, one-way ANOVA with Tukey's post hoc test (between strains) and two-sample t test (control versus pregabalin treatment).

3D, whole-brain perspective with a high temporal resolution. This methodology has permitted further insight into the spatiotemporal dynamics of SD in both WT mice and those displaying mild (R192Q) or severe (S218L) FHM-1 phenotypes (7). Further, we tested the hypothesis that pregabalin, an antiepileptic with high-affinity binding to $\alpha_2\delta_1$-containing calcium channel complexes, may exhibit functional effects in FHM-1 and WT mice. Our key findings concerning SD and the actions of pregabalin are (*i*) SD threshold and speed are differentially affected by R192Q and S218L FHM-1 mutations; (*ii*) in both FHM-1 strains SD invades the striatum and hippocampus, albeit with a notable delay in R192Q animals; (*iii*) SD does not invade the cerebellum in any strain or under any stimulation protocol; (*iv*) the SD threshold is increased by pregabalin in WT but not in FHM-1 mice; (*v*) pregabalin slows SD velocity in both FHM-1 strains but not WT mice; and (*vi*) SD invasion of subcortical structures is suppressed by pregabalin in animals expressing the milder R192Q change but not in animals expressing the more severe S218L FHM-1 mutation.

SD Threshold and Speed Are Differentially Affected by the R192Q and S218L FHM-1 Mutations. We observed a lower SD threshold in vivo in S218L mice than in WT and R192Q animals, suggesting that only the S218L $Ca_V2.1$ channel gain-of-function mutation was sufficiently pathophysiological to promote the initiation of SD as a result of cortical electrical depolarization. This finding was somewhat unexpected because previous data indicated a lowered SD threshold associated with both FHM-1 mutations (8, 9) and also because both R192Q and S218L mice display enhanced glutamatergic activity in cortical neurons (15, 16, 32). Notably, the use of isoflurane (instead of urethane) in the current study may have differentially affected the SD threshold. Also, the carbon fiber electrodes used for stimulation in the MRI scanner are larger in diameter than the metal electrodes used previously, and this difference may have affected stimulation sensitivity (9). If the stimulation threshold is modulated solely by the level of synaptic excitability, a lower SD threshold would be expected in both S218L and R192Q mice. Our findings may indicate that the SD threshold is not linked directly to synaptic activity but instead is linked to enhanced basal neuronal excitability in the cortex. This notion fits with previous data demonstrating that cortical neurons from S218L mice display calcium currents with a distinct leftward shift in activation properties that is less pronounced in R192Q mice (16). As a result, S218L neurons are predicted to have the ability to conduct calcium at rest, endowing them with the ability to modulate neuronal excitability at a range of membrane potentials normally considered subthreshold (13).

Although the SD threshold was found to be decreased only in S218L animals, we observed an increase in cortical SD conduction velocity, similar to that described previously (8, 9), in both R192Q and S218L FHM-1 strains. The gain-of-function alterations of $Ca_V2.1$ channels containing R192Q or S218L mutations likely

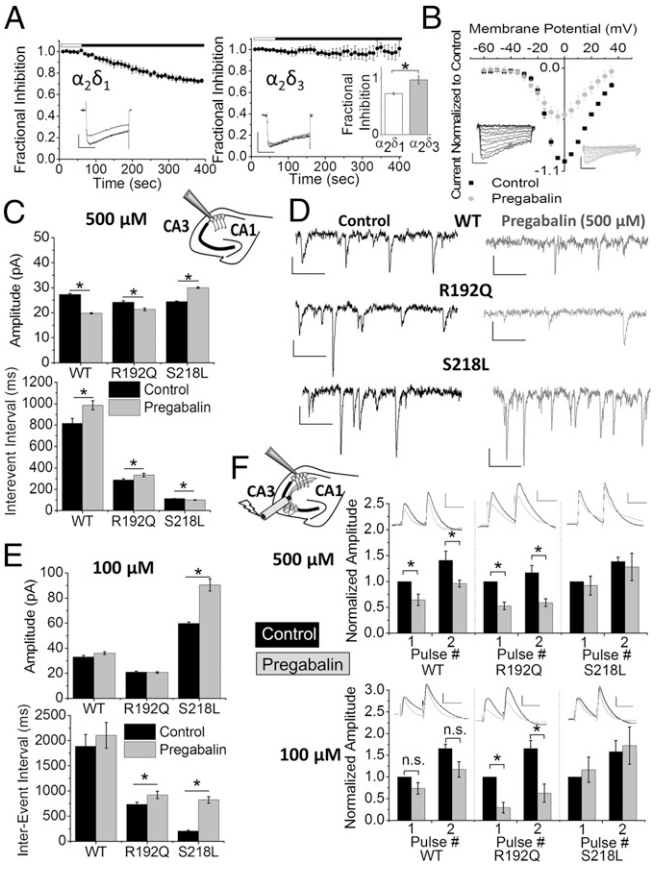

Fig. 5. Pregabalin acutely inhibits $Ca_V2.1$ Ca^{2+} currents and both spontaneous and evoked synaptic activity. (*A*) Time course of pregabalin (500 μM) on currents recorded from SH-SY5Y cells cotransfected with the $Ca_V2.1$ α_1,β_4 and $\alpha_2\delta_1$ (n = 8) (*Left*) or with $\alpha_2\delta_3$ (n = 4) (*Right*) subunits. *Insets* show representative currents (black, control; grey, pregabalin) and mean fractional inhibition (*Right*). (*B*) Mean $Ca_V2.1$ current density–voltage relationships obtained before and after the application of pregabalin. *Insets* show representative currents. (*C*) Schematic of acute hippocampal brain slice preparation used in *C*–*E* for whole-cell voltage-clamp recordings in CA1 neurons. Shown are mean data for the effect of 500 μM pregabalin on sEPSC amplitude (*Upper*) and the interevent interval (*Lower*); WT: n = 7 cells, 4 animals; R192Q: n = 6 cells, 4 animals; S218L: n = 9 cells, 4 animals. (*D*) Representative current traces taken from 60-s voltage-clamp recordings at CA1 soma showing the effect of pregabalin (500 μM) on sEPSCs in WT, R192Q, and S218L FHM-1 strains. (Scale bars: horizontal, 100 ms; vertical 10 pA.) (*E*) Mean data for the effect of 100 μM pregabalin on sEPSC amplitude (*Upper*) and the interevent interval (*Lower*); WT: n = 5 cells, 3 animals; R192Q: n = 4 cells, 3 animals; S218L: n = 5 cells, 3 animals. (*F*, *Upper Left*) Schematic of slice preparation used in whole-cell current-clamp recordings in CA1 neurons with paired (1-ms pulse, 67-ms interval) stimulation applied to CA3 axons. (*Upper Right*) Mean data for eEPSP amplitude in response to 500 μM pregabalin; WT: n = 6 cells, 4 animals; R192Q: n = 6 cells, 4 animals; S218L: n = 8 cells, 4 animals. (*Lower*) Mean data for eEPSP amplitude in response to 100 μM pregabalin; WT: n = 5 cells, 3 animals; R192Q: n = 4 cells, 3 animals; S218L: n = 5 cells, 3 animals. *Insets* show representative eEPSPs from WT, R192Q, and S218L CA1 neurons (black, control; grey, pregabalin); WT: n = 6 cells, 4 animals; R192Q: n = 6 cells, 4 animals; S218L: n = 8 cells, 4 animals. (*Inset* scale bars: horizontal, 50 ms; vertical, 5 mV.) *P < 0.05.

underlie the observed increases in SD speed in these strains; this possibility is supported by studies demonstrating enhanced synaptic activity in cortical neurons from both R192Q (15, 32) and S218L mice (16).

SD Spreads to Subcortical Structures in Both FHM-1 Strains but Not in WT Mice. Several mechanisms, such as interneuronal-mediated signaling or passive diffusion of neuroactive substances through extracellular fluid (5), have been proposed to contribute to the spread of SD. In R192Q mice, a progressive spread of SD to subcortical structures was observed particularly in slice 5 (bregma −2.50 mm). Typically, the SD propagated ventrolaterally from the dorsomedial cortex until reaching the entorhinal cortex, followed by the delayed appearance of SD first in the ventral hippocampus and then in the dorsal hippocampus. Similarly, this pattern of SD propagation was observed in slice 6 in R192Q mice, with SD spreading into the striatum (Figs. 2 and 3 and Movie S3). These results suggest that failure-points where SD propagation is limited normally exist between certain interconnected areas, for example the entorhinal cortex–subiculum and piriform cortex–striatum, and that a diffusional and/or synaptic barrier must be bridged for SD to spread further. We speculate that neurons expressing $Ca_V2.1$ channels containing either R192Q or S218L mutations enable the spread of SD across subcortical failure-points.

Hippocampal SD has been reported previously after direct stimulation of the CA1 region in Sprague–Dawley rats (33), indicating that SD can indeed be initiated in this brain region but likely does not receive sufficient input during cortical SD and/or that a barrier in this region prevents the propagation of cortically initiated SD. Invasion of SD into the striatum has been observed in some rat models (34), and in our IOS slice preparation we regularly observed SD invasion and initiation in the striatum of WT mice. Because WT animals did not display subcortical SD in vivo, it is likely that, like the hippocampus, the striatum is capable of SD but cannot normally propagate the wave in response to adjacent cortical SD. It has been suggested that in FHM-1 mice SD may spread to the striatum and hippocampus via the amygdala and subiculum, respectively, and that lower neuronal densities in these areas may be responsible for limiting SD spread in WT animals (28). Our data from R192Q animals support this view with respect to the anatomical entry point of SD into these structures for this strain. In S218L mice, in which SD spreads immediately from the adjacent cortex to subcortical structures, the stronger gain-of-function effect of the mutation on $Ca_V2.1$ channels apparently generates an SD wave that is sufficiently powerful to traverse the corpus callosum. Of further interest is that SD is not observed to propagate into the thalamus for either of the FHM-1 mutations, although this propagation has been reported to occur in a percentage of S218L mice (28). It should be considered that in the study by Eikermann-Haerter et al. (28) the electrophysiological measurements of SD were made under pentobarbital anesthesia, whereas our experiments were performed under isoflurane anesthesia; the two anesthetics may have distinct effects on SD invasion into the thalamus (35). Despite this difference, both studies indicate that the white matter of the internal capsule appears to be a particularly difficult region for SD to traverse.

It is noteworthy that we did not observe SD in the cerebellum, even when stimulation electrodes were placed directly into the cerebellar cortex. In agreement with our findings, cerebellar SD has not been reported previously in the FHM-1 mouse strains, although it has been observed in rats (36). Strong cerebellar symptoms in FHM-1 patients, including those with the S218L mutation, are well described, and altered synaptic activity has been reported in cerebellar synapses in S218L mice (12, 37). Our results suggest that the FHM-1–mediated cerebellar symptoms are not associated with functional changes that might occur as a result of any recurrent SD within the cerebellum.

SD Threshold Is Increased by Pregabalin in WT but Not in FHM-1 Mice. Gabapentin has been shown to increase the threshold for SD in vivo (38), and we hypothesized that pregabalin also might alter SD. Furthermore, gabapentin and pregabalin are known to bind to the $\alpha_2\delta_{1/2}$ auxiliary subunit of $Ca_V2.1$ calcium channels, and gabapentinoid-mediated inhibition of calcium currents has been reported both acutely (24, 30, 39) and via chronic effects on channel trafficking (25, 40). In the current study pregabalin was effective in increasing the threshold for stimulation to induce SD in WT but not R192Q or S218L mice. This finding suggests that pregabalin may be an effective treatment for preventing migraine with aura in migraineurs without FHM-1 mutations. In contrast, in FHM-1 patients the gain-of-function phenotypes conferred to $Ca_V2.1$ channels may be too severe for pregabalin to be therapeutically efficacious. We did, however, observe a trend toward increased threshold following acute pregabalin treatment in FHM-1 mice, and therefore pregabalin should not necessarily be ruled out as a chronically administered preventative treatment for FHM-1 patients.

Pregabalin Slows SD in FHM-1 Strains but Not in WT Mice. We demonstrated that pregabalin slowed SD in S218L and R192Q but not WT mice. As discussed, cortical synapses that express $Ca_V2.1$ channels containing the R192Q and S218L mutations display enhanced excitatory, but not inhibitory, neurotransmission (16, 32), and a leftward shift in the activation curve of $Ca_V2.1$ channels containing the S218L mutation allows calcium conduction at resting membrane potentials (16). Together these characteristics would permit subthreshold modulation of excitability by $Ca_V2.1$ in S218L mice, providing a potential mechanism underlying the more severe phenotype in this strain. Pregabalin has a direct inhibitory effect on calcium-mediated glutamate release in brain slices from neocortex (41) and entorhinal cortex (42). In addition, pregabalin displays two- to threefold enhanced efficacy in the depression of noradrenaline release upon sustained depolarization as compared with brief stimulation (26, 43). The long-lasting depolarization that occurs during SD may further increase the efficacy of pregabalin on neurotransmitter release when attenuating the synaptic gain of function resulting from R192Q and S218L mutations. Overall, pregabalin's greater effectiveness in slowing SD speed in FHM-1 mice than in WT mice directly supports our hypothesis that pregabalin has a functional inhibitory effect on native $Ca_V2.1$ channels.

SD Invasion of Subcortical Structures Is Abolished by Pregabalin in R192Q Mice. A notable finding from our DW-MRI experiments is that pregabalin prevented the subcortical invasion of SD in four of five R192Q animals. Given that pregabalin did not prevent subcortical invasion in S218L mice, we would argue that pregabalin suppresses excitability sufficiently to prevent SD propagation through failure points that block the spread of SD into subcortical structures in the milder R192Q phenotype mice. Previous studies have demonstrated that pregabalin inhibits vesicle trafficking in hippocampal neurons, reducing the readily releasable pool (44) and attenuating vesicle release (45). In hippocampal brain slices, we observed that pregabalin (500 μM) effectively suppressed both spontaneous and evoked synaptic activity in WT and R192Q CA1 neurons but not in S218L CA1 neurons. This strain-specific inhibition of evoked synaptic function provides a molecular mechanism for pregabalin to suppress the invasion of the hippocampus in R192Q mice but not in S218L mice. Although SD did not invade the hippocampus spontaneously in WT mice, pregabalin's efficacy on synaptic activity in WT CA1 neurons suggests that it may provide an effective preventative treatment to limit the subcortical progression of migraine in non–FHM-1 migraineurs and in milder forms of FHM-1.

In summary, we find that SD is limited to defined brain regions by as yet unknown synaptic and/or diffusional barriers involving $Ca_V2.1$ (P/Q-type) calcium channel-mediated excitability and that these barriers can be bridged by the consequences of FHM-1 mutations. Furthermore, pregabalin is effective in increasing the threshold for SD in WT animals, in slowing SD velocity in FHM-1 mice, and in preventing SD subcortical propagation associated with the milder R192Q FHM-1 mutation. These findings support the notion that pregabalin may be effective acutely but have

not addressed its effects with chronic drug administration. Although gabapentin has recently fallen from favor as a preventative treatment in migraine (19), initial reports on the use of pregabalin are encouraging (21–23). The current study provides insights into the mechanism of action of pregabalin and supports its therapeutic potential in both non-FHM migraineurs and patients with milder FHM-1 mutations.

Materials and Methods

Full details on methods used for DW-MRI, brain slice IOS, cell culture, and electrophysiology can be found in *SI Materials and Methods*. All experiments were performed in accordance with the guidelines of the Canadian Council on Animal Care and the University of British Columbia Animal Care Committee (see *SI Materials and Methods*).

ACKNOWLEDGMENTS. This work was supported by a Brain Canada Multi-Investigator Research Initiative Grant with matching support from Genome BC, the Michael Smith Foundation for Health Research, and the Koerner Foundation. T.P.S. and S.M.C. were supported by a Pfizer Neuropathic Pain Award. T.P.S. also was supported by Canadian Institutes of Health Research (CIHR) Operating Grant 10677 and by the Canadian Research Chair (CRC) in Biotechnology and Genomics-Neurobiology. S.M.C. was supported by a research grant from the BC Epilepsy Society. B.A.M. was supported by a CRC in Neuroscience, CIHR Operating Grants 148397, 8545, and 115121, TCE-117869 in the framework of European Research Area Networks NEURON, and the Fondation Leducq.

1. Headache Classification Committee of the International Headache Society (IHS) (2013) The international classification of headache disorders, 3rd edition (beta version). *Cephalalgia* 33(9):629–808.
2. Dreier JP (2011) The role of spreading depression, spreading depolarization and spreading ischemia in neurological disease. *Nat Med* 17(4):439–447.
3. Hadjikhani N, et al. (2001) Mechanisms of migraine aura revealed by functional MRI in human visual cortex. *Proc Natl Acad Sci USA* 98(8):4687–4692.
4. Lauritzen M, et al. (2011) Clinical relevance of cortical spreading depression in neurological disorders: Migraine, malignant stroke, subarachnoid and intracranial hemorrhage, and traumatic brain injury. *J Cereb Blood Flow Metab* 31(1):17–35.
5. Pietrobon D, Moskowitz MA (2014) Chaos and commotion in the wake of cortical spreading depression and spreading depolarizations. *Nat Rev Neurosci* 15(6): 379–393.
6. Karatas H, et al. (2013) Spreading depression triggers headache by activating neuronal Panx1 channels. *Science* 339(6123):1092–1095.
7. Ferrari MD, Klever RR, Terwindt GM, Ayata C, van den Maagdenberg AMJM (2015) Migraine pathophysiology: Lessons from mouse models and human genetics. *Lancet Neurol* 14(1):65–80.
8. van den Maagdenberg AM, et al. (2004) A Cacna1a knockin migraine mouse model with increased susceptibility to cortical spreading depression. *Neuron* 41(5):701–710.
9. van den Maagdenberg AM, et al. (2010) High cortical spreading depression susceptibility and migraine-associated symptoms in Ca(v)2.1 S218L mice. *Ann Neurol* 67(1):85–98.
10. Adams PJ, et al. (2009) Ca(V)2.1 P/Q-type calcium channel alternative splicing affects the functional impact of familial hemiplegic migraine mutations: Implications for calcium channelopathies. *Channels (Austin)* 3(2):110–121.
11. Tottene A, et al. (2005) Specific kinetic alterations of human CaV2.1 calcium channels produced by mutation S218L causing familial hemiplegic migraine and delayed cerebral edema and coma after minor head trauma. *J Biol Chem* 280(18):17678–17686.
12. Adams PJ, et al. (2010) Contribution of calcium-dependent facilitation to synaptic plasticity revealed by migraine mutations in the P/Q-type calcium channel. *Proc Natl Acad Sci USA* 107(43):18694–18699.
13. Di Guilmi MN, et al. (2014) Synaptic gain-of-function effects of mutant Cav2.1 channels in a mouse model of familial hemiplegic migraine are due to increased basal [Ca2+]i. *J Neurosci* 34(21):7047–7058.
14. Kaja S, et al. (2010) Severe and progressive neurotransmitter release aberrations in familial hemiplegic migraine type 1 Cacna1a S218L knock-in mice. *J Neurophysiol* 104(3):1445–1455.
15. Tottene A, et al. (2009) Enhanced excitatory transmission at cortical synapses as the basis for facilitated spreading depression in Ca(v)2.1 knockin migraine mice. *Neuron* 61(5):762–773.
16. Vecchia D, Tottene A, van den Maagdenberg AMJM, Pietrobon D (2015) Abnormal cortical synaptic transmission in CaV2.1 knockin mice with the S218L missense mutation which causes a severe familial hemiplegic migraine syndrome in humans. *Front Cell Neurosci* 9:8.
17. Gelfand AA, Goadsby PJ (2012) A neurologist's guide to acute migraine therapy in the emergency room. *Neurohospitalist* 2(2):51–59.
18. Li Z, et al. (2011) Pregabalin is a potent and selective ligand for α(2)δ-1 and α(2)δ-2 calcium channel subunits. *Eur J Pharmacol* 667(1-3):80–90.
19. Linde M, Mulleners WM, Chronicle EP, McCrory DC (2013) Gabapentin or pregabalin for the prophylaxis of episodic migraine in adults. *Cochrane Database Syst Rev* 6(6): CD010609.
20. Bockbrader HN, et al. (2010) A comparison of the pharmacokinetics and pharmacodynamics of pregabalin and gabapentin. *Clin Pharmacokinet* 49(10):661–669.
21. Bakhshandeh Bali M, et al. (2015) Comparison of propranolol and pregabalin for prophylaxis of childhood migraine: A randomised controlled trial. *Acta Med Iran* 53(5):276–280.
22. Calandre EP, Garcia-Leiva JM, Rico-Villademoros F, Vilchez JS, Rodriguez-Lopez CM (2010) Pregabalin in the treatment of chronic migraine: An open-label study. *Clin Neuropharmacol* 33(1):35–39.
23. Pizzolato R, Villani V, Prosperini L, Ciuffoli A, Sette G (2011) Efficacy and tolerability of pregabalin as preventive treatment for migraine: A 3-month follow-up study. *J Headache Pain* 12(5):521–525.
24. Uchitel OD, Di Guilmi MN, Urbano FJ, Gonzalez-Inchauspe C (2010) Acute modulation of calcium currents and synaptic transmission by gabapentinoids. *Channels (Austin)* 4(6):490–496.
25. Bauer CS, et al. (2010) The anti-allodynic alpha(2)delta ligand pregabalin inhibits the trafficking of the calcium channel alpha(2)delta-1 subunit to presynaptic terminals in vivo. *Biochem Soc Trans* 38(2):525–528.
26. Dooley DJ, Donovan CM, Meder WP, Whetzel SZ (2002) Preferential action of gabapentin and pregabalin at P/Q-type voltage-sensitive calcium channels: Inhibition of K+-evoked [3H]-norepinephrine release from rat neocortical slices. *Synapse* 45(3): 171–190.
27. Dworkin RH, Kirkpatrick P (2005) Pregabalin. *Nat Rev Drug Discov* 4(6):455–456.
28. Eikermann-Haerter K, et al. (2011) Enhanced subcortical spreading depression in familial hemiplegic migraine type 1 mutant mice. *J Neurosci* 31(15):5755–5763.
29. Zhou N, Gordon GRJ, Feighan D, MacVicar BA (2010) Transient swelling, acidification, and mitochondrial depolarization occurs in neurons but not astrocytes during spreading depression. *Cereb Cortex* 20(11):2614–2624.
30. Di Guilmi MN, Urbano FJ, Inchauspe CG, Uchitel OD (2011) Pregabalin modulation of neurotransmitter release is mediated by change in intrinsic activation/inactivation properties of Ca(v)2.1 calcium channels. *J Pharmacol Exp Ther* 336(3):973–982.
31. Marais E, Klugbauer N, Hofmann F (2001) Calcium channel alpha(2)delta subunits-structure and Gabapentin binding. *Mol Pharmacol* 59(5):1243–1248.
32. Vecchia D, Tottene A, van den Maagdenberg AMJM, Pietrobon D (2014) Mechanism underlying unaltered cortical inhibitory synaptic transmission in contrast with enhanced excitatory transmission in CaV2.1 knockin migraine mice. *Neurobiol Dis* 69:225–234.
33. Herreras O, Largo C, Ibarz JM, Somjen GG, Martín del Río R (1994) Role of neuronal synchronizing mechanisms in the propagation of spreading depression in the in vivo hippocampus. *J Neurosci* 14(11 Pt 2):7087–7098.
34. Vinogradova LV, Koroleva VI, Bures J (1991) Re-entry waves of Leao's spreading depression between neocortex and caudate nucleus. *Brain Res* 538(1):161–164.
35. Takagaki M, et al. (2014) Isoflurane suppresses cortical spreading depolarizations compared to propofol–implications for sedation of neurocritical care patients. *Exp Neurol* 252:12–17.
36. Fifkova E, Bures J, Koshtoyants OK, Krivanek J, Weiss T (1961) Leao's spreading depression in the cerebellum of rat. *Experientia* 17:572–573.
37. Gao Z, et al. (2012) Cerebellar ataxia by enhanced Ca(V)2.1 currents is alleviated by Ca2+-dependent K+-channel activators in Cacna1a(S218L) mutant mice. *J Neurosci* 32(44):15533–15546.
38. Hoffmann U, Dileköz E, Kudo C, Ayata C (2010) Gabapentin suppresses cortical spreading depression susceptibility. *J Cereb Blood Flow Metab* 30(9):1588–1592.
39. Weissmann C, Di Guilmi MN, Urbano FJ, Uchitel OD (2013) Acute effects of pregabalin on the function and cellular distribution of Ca(V)2.1 in HEK293t cells. *Brain Res Bull* 90:107–113.
40. Dolphin AC (2012) Calcium channel auxiliary α2δ and β subunits: Trafficking and one step beyond. *Nat Rev Neurosci* 13(8):542–555.
41. Fink K, et al. (2002) Inhibition of neuronal Ca(2+) influx by gabapentin and pregabalin in the human neocortex. *Neuropharmacology* 42(2):229–236.
42. Cunningham MO, Woodhall GL, Thompson SE, Dooley DJ, Jones RSG (2004) Dual effects of gabapentin and pregabalin on glutamate release at rat entorhinal synapses in vitro. *Eur J Neurosci* 20(6):1566–1576.
43. Dooley DJ, Donovan CM, Pugsley TA (2000) Stimulus-dependent modulation of [(3)H]norepinephrine release from rat neocortical slices by gabapentin and pregabalin. *J Pharmacol Exp Ther* 295(3):1086–1093.
44. Holz RW (2006) Pharmacology meets vesicular trafficking at a central nervous system synapse: Pregabalin effects on synaptic vesicle cycling in hippocampal neurons. *Mol Pharmacol* 70(2):444–446.
45. Micheva KD, Taylor CP, Smith SJ (2006) Pregabalin reduces the release of synaptic vesicles from cultured hippocampal neurons. *Mol Pharmacol* 70(2):467–476.
46. de Crespigny A, Röther J, van Bruggen N, Beaulieu C, Moseley ME (1998) Magnetic resonance imaging assessment of cerebral hemodynamics during spreading depression in rats. *J Cereb Blood Flow Metab* 18(9):1008–1017.
47. Vartanian MG, et al. (2006) Activity profile of pregabalin in rodent models of epilepsy and ataxia. *Epilepsy Res* 68(3):189–205.
48. Lein ES, et al. (2007) Genome-wide atlas of gene expression in the adult mouse brain. *Nature* 445:168–176.